International Journal of Theoretical Physics, Vol. 28, No. 3, 1989

Particle Decay Model

Stanley Gudder[1]

Received November 20, 1988

Applying a finite color symmetry group, it is shown that every "elementary particle" can be associated with a unique graph. This graph describes the gluon motions and is called the particle's strong graph. One also has an associated weak graph that describes the photon motions. Using the strong (weak) graph, one can exhibit the various strong (weak) decay modes of a particle. Roughly speaking, the particle graph disintegrates into smaller graphs that represent the decay products. The disintegration is dictated by certain decay operations and these operations have specified probability costs. The costs are then used to predict branching ratios and decay probabilities. For the examples presented, these predictions agree with experiment to within 1%.

1. INTRODUCTION

In a previous work (Gudder, 1988), I presented a finite model for "elementary particles." In this model, each particle is represented by a graph. The vertices of the graph correspond to quarklike constituents and the edges correspond to gluon or photon paths. The gluons and photons perform a quantum random walk along the specified paths that is governed by a unitary absorption-emission matrix. In fact, the entries of this matrix are transition amplitudes that are discrete analogs of continuum Feynman transition amplitudes. The possible gluon and photon energy values were computed in terms of the eigenvalues of the absorption-emission matrix. I then postulated certain mass formulas in terms of these energy values and the structure of the corresponding graph. The mass formulas gave predicted particle masses that closely agreed with experiment for a large number of particles.

The present paper applies this model to the study of particle decay. I first derive the strong particle graphs by postulating a certain finite color

[1]Department of Mathematics and Computer Science, University of Denver, Denver Colorado 80208.

0020-7748/89/0300-0273S06.00/0

symmetry group. The weak and strong decays are described by a disintegration of the graphs into smaller graphs that represent decay products. Each step in the disintegration has a specified probability cost. These costs are used to predict branching ratios and decay probabilities. Sections 2 and 3 treat strong and weak graphs, respectively, while Sections 4–6 consider weak baryon, weak meson, and strong baryon decays, respectively. Some concluding remarks are given in Section 7.

2. STRONG GRAPHS

As with most elementary particle studies, a symmetry group plays a basic role in this model. However, unlike the traditional theories, this is a finite model and the symmetry group is a small finite group. In fact, it is the smallest non-abelian group, namely the dihedral group D_3 (or the symmetric group S_3).

Let us first consider the strong graph associated with a particle. Since the strong interaction is a "color" interaction, let us begin with the set of color charges

$$S = \{r, y, b, \bar{r}, \bar{y}, \bar{b}\}.$$

There are two important bijections on S, the color rotation $c: S \to S$ defined by

$$c(r) = y, \qquad c(y) = b, \qquad c(b) = r, \qquad c(\bar{r}) = \bar{b}, \qquad c(\bar{y}) = \bar{r}, \qquad c(\bar{b}) = \bar{y}$$

and the color-anticolor flip $f: S \to S$ defined by

$$f(x) = \bar{x}, \qquad f(\bar{x}) = x, \qquad x \in S$$

If we denote the compositions by juxtaposition and denote the identity function by e, then f and c satisfy

$$f^2 = ff = e, \qquad c^3 = e, \qquad cf = fc^2 \tag{1}$$

It then follows that c and f are the generators of a group G of bijections on S. In fact, G is isomorphic to the symmetric group S_3 of all bijections on a three-element set, which, in this case, coincides with the dihedral group D_3 of order 6. This is easily seen from Table I, which is the group table

Table I. Group Table

	e	c	c^2	f	fc	cf
e	e	c	c^2	f	fc	cf
c	c	c^2	c	cf	f	fc
c^2	c^2	e	c	fc	cf	f
f	f	fc	cf	e	c	c^2
fc	fc	cf	f	c^2	e	c
cf	cf	f	fc	c	c^2	e

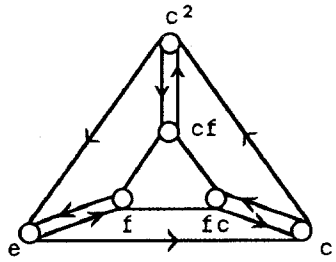

Fig. 1. Cayley graph for G.

for G. Table I can be constructed directly or more easily by applying equation (1). A useful way of picturing a finite group is given in terms of its Cayley graph. The vertices of the Cayley graph represent group elements and directed edges of the graph represent the actions of a minimal set of generators for the group. The Cayley graph for our group G is illustrated in Figure 1. In Figure 1 the edges of the two triangles represent the action of c and the three double edges represent the action of f.

Another way to picture G is to diagram the actions of the functions c and f on the set S as illustrated in Figure 2. In this figure, the three vertices represent color-anticolor pairs $(r, \bar{r})$, $(y, \bar{y})$, $(b, \bar{b})$. The outer edges of the triangle represent the action of c on the first argument of a pair and the inner edges of the triangle represent the action of c on the second argument. The left loop of a loop pair represents the action of f on the first argument and the right loop represents the action of f on the second argument.

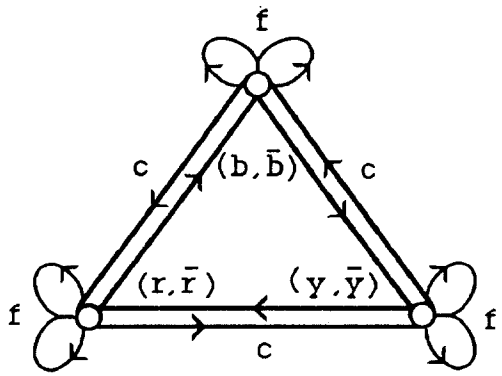

Fig. 2. Graph for G.

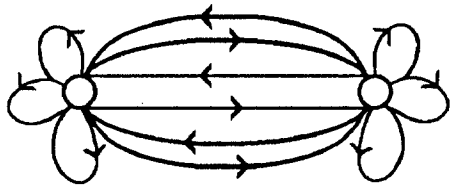

Fig. 3. Identified vertices.

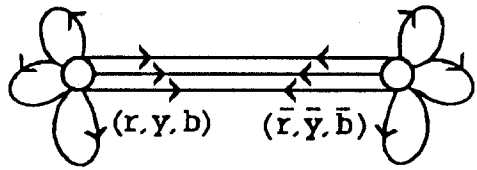

Fig. 4. Another graph for G.

Notice that Figure 2 is obtained from Figure 1 by identifying the vertices in the pairs (e,f), (c,fc), (c^2, cf). We can obtain another description of G from Figure 1 by identifying the vertices e, c, c^2 and f, fc, cf. This is illustrated in Figure 3. A more economical way of depicting Figure 3 in accordance with the actions of c and f on S is illustrated in Figure 4. Figures 2 and 4 will be useful in our study of elementary particles.

Let us assume that the graphs in Figures 2 and 4 represent elementary particles. The vertices of these graphs represent quarklike constituents of the particles. Since interactions in nature are not caused by functions such as c and f, but are mediated by particles, assume that the edges of these graphs represent interaction paths for gluons. If we strip the vertices of their labels and the edges of their arrows, we obtain the graphs M and B in Figure 5.

I call subgraphs of M *meson graphs* and subgraphs of B are called *baryon graphs.* Now there are many meson and baryon graphs that do not correspond to actual particles. In order to restrict the number of possibilities, I introduce two important properties of the vertices. Each vertex of a meson

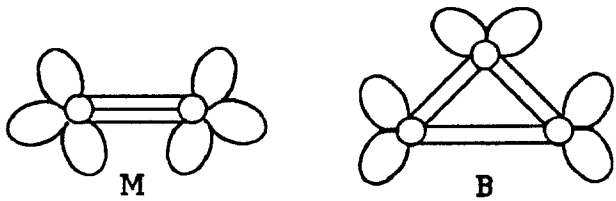

Fig. 5. Graphs M and B.

or baryon graph has an (electric) charge $\pm 1/3$ or $\pm 2/3$ and a (z component of) spin $\pm 1/2$ (up, down). I now postulate the following charge rules.

(C1) The sum of the charges is integral.

(C2) If a vertex has an odd number of loops, then its charge is $\pm 1/3$ and if a vertex has an even nonzero number of loops, then its charge is $\pm 2/3$.

Rule C1 is a standard property for quark models and Rule C2 gives the usual quark and lepton generations. I next postulate the following meson spin rules.

(M1) The two vertices have opposite spin if and only if they are joined by one or two edges. They have the same spin if and only if they are joined by three edges.

(M2) For opposite spin, if both vertices have at least one loop, then they are joined by two edges and if exactly one vertex has at least one loop, then they are joined by one edge.

As shown in Gudder (1988), more edges give higher energies. Rule M1 now follows from the fact that it takes more energy to keep spins aligned than disaligned. Rule M2 indicates that in the opposite-spin case, more energy is required when both vertices have loops than if just one does.

Finally, I postulate the baryon spin rules.

(B1) Two vertices have opposite spin if and only if they are joined by one edge and they have the same spin if and only if they are joined by two edges.

(B2) If two vertices have the same charge and the same number of loops, then they have the same spin.

Rule B1 follows from the same reasoning as Rule M1. Rule B2 is a graph-theoretic exclusion principle analogous to antisymmetric fermion states. A meson graph that obeys Rules C1, C2, M1, and M2 is called *admissible* meson graph. A baryon graph that obeys Rules C1, C2, B1, and B2 is called an *admissible* baryon graph.

It turns out that there is a one-to-one correspondence between meson isospin multiplets and admissible meson graphs. Figure 6 exhibits this correspondence for the established meson isospin multiplets. In this figure an open circle represents a vertex with spin $1/2$ and a filled circle represents a vertex with spin $-1/2$.

Notice that in this model, edges between different vertices correspond to strong interactions and loops correspond to weak interactions. Moreover, one loop corresponds to strange quarks, two to charmed quarks, and three to bottom quarks. In a similar way, there is a one-to-one correspondence between baryon isospin multiplets and admissible baryon graphs. These are exhibited in Figure 7 for the established baryons.

The standard quark model postulates the existence of further quark constituents such as the top quark. Such quarks would require four or more

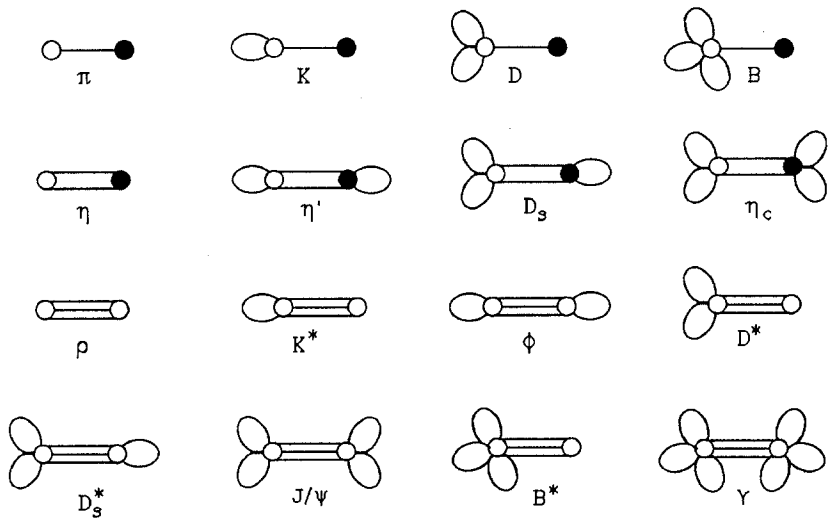

Fig. 6. Admissible meson graphs.

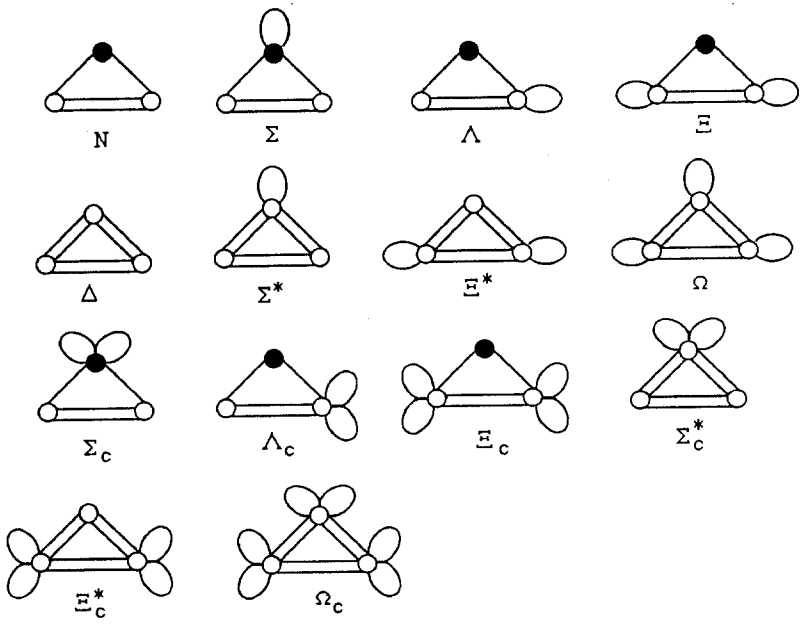

Fig. 7. Admissible baryon graphs.

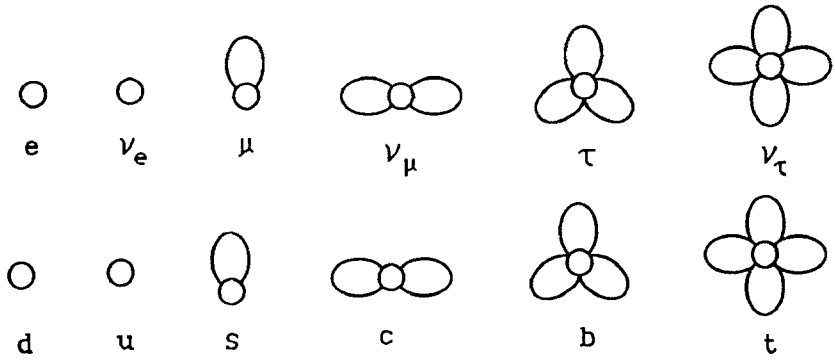

Fig. 8. Lepton and quark graphs.

loops. These can be accommodated in the present model, if necessary, by including more colors and, hence, more loops. For completeness, I illustrate graphs for leptons and quarks in Figure 8. These are point particles with just one vertex and the usual charges.

I call the graphs in Figures 6 and 7 *strong* graphs. I have not yet designated the electric charge for vertices of strong graphs. If this is done in accordance with the previous rules, then the usual isospin multiplet structure results. This is illustrated in Figure 9 for the first few baryons. Similar graphs can be constructed for the mesons. In the sequel I shall frequently only consider particles, since their corresponding antiparticles are obtained in the standard way by negating all charges. Moreover, if we flip all spins, the particle (or graph) is considered to be the same.

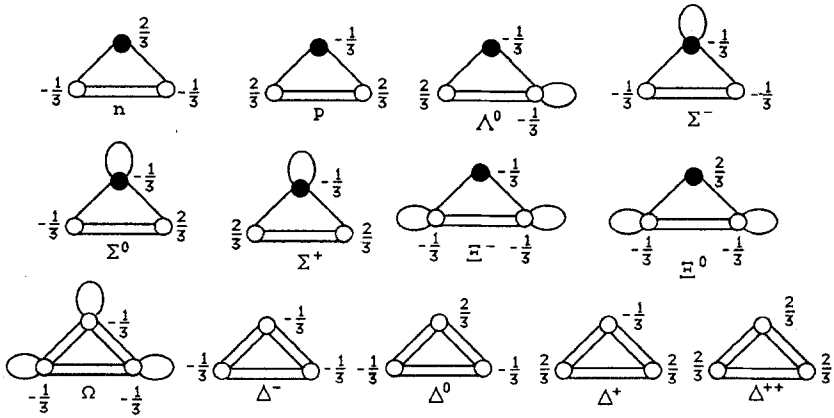

Fig. 9. Multiplet structure.

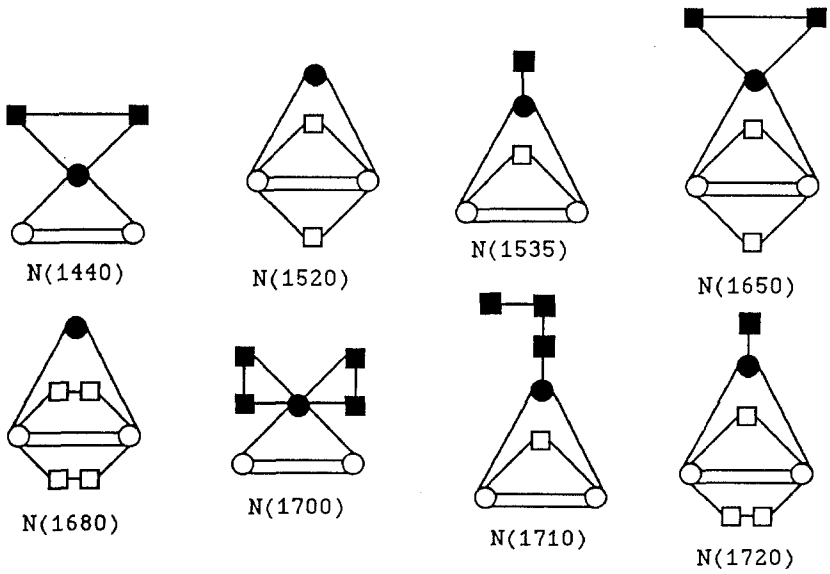

Fig. 10. Excited baryons.

Until now I have considered what I call *basic* mesons and baryons. To account for the other known particles one must also consider *excited* mesons and baryons. The graphs of these excited particles are obtained by adjoining pairs of new vertices that I call *excitation vertices* to the graphs of the basic particles. The additional edges are called *excitation edges.* The excitation vertices must be adjoined according to certain rules (Gudder, 1988). Figure 10 illustrates some excited nucleons. In this figure excitation vertices are denoted by open squares (spin 1/2) and filled squares (spin $-1/2$). Other excited particle graphs are obtained in a similar way (Gudder, 1988).

3. WEAK GRAPHS

The edges and loops in the strong graphs of Section 2 represented gluon paths. However, due to electroweak interactions, one also has photon paths (there is no need to postulate the existence of weak gauge bosons in this model). I could adjoin new edges to the strong graph to represent these photon paths; but for simplicity I shall construct a new graph which I call a *weak graph.* The weak graph for a particle has the same vertices and loops as the strong graph but the edges joining distinct vertices are different. For weak meson graphs I postulate the following rule (Gudder, 1988) (see Figure 11 for illustrations).

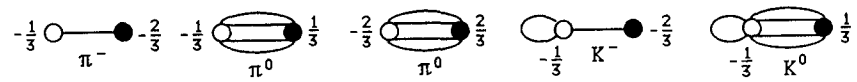

Fig. 11. Weak meson graphs.

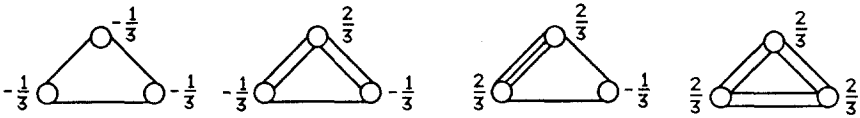

Fig. 12. Even number of loops.

(WM) if the electric charges of the two vertices have the same sign, they are joined by one edge. If they have opposite sign, they are joined by four edges.

For weak baryon graphs one has the following rule (Gudder, 1988).

(WB) If the baryon contains an even (odd) number of loops, the weak graph has the form exhibited in Figure 12 (Figure 13).

Note that Figures 12 and 13 are the same except $-1/3$ and $2/3$ are interchanged. In Figures 12 and 13 I have ignored the spin and the loops of the baryon, which can be arbitrary if they do not violate any of the rules. Figure 14 illustrates some weak baryon graphs. Since the leptons only have loops, their weak and strong graphs are identical.

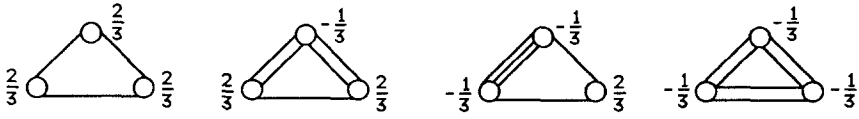

Fig. 13. Odd number of loops.

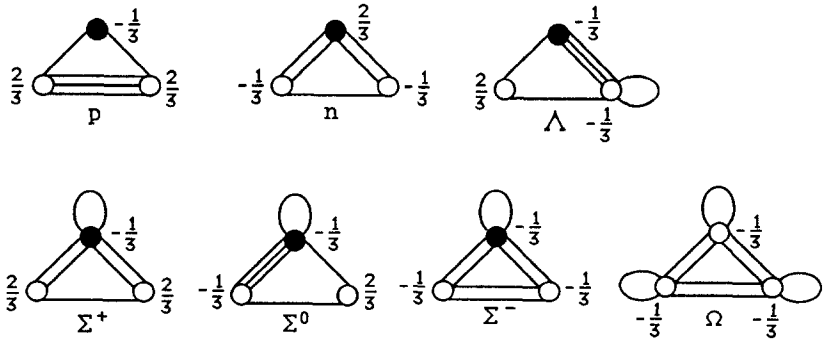

Fig. 14. Weak baryon graphs.

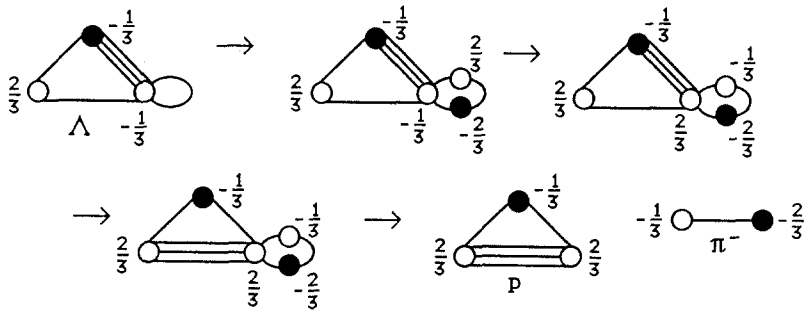

Fig. 15. $\Lambda \to p\pi^-$.

4. WEAK BARYON DECAY

Suppose we have a weak decay process $A \to BC$ in which a baryon A decays weakly into two particles B and C. I shall describe this process in terms of the weak graphs of A, B, and C. Roughly speaking, the weak graph of A first inflates to accommodate new vertices and then disintegrates into two components corresponding to the weak graphs of B and C. Figures 15 and 16 illustrate the weak processes $\Lambda \to p\pi^-$ and $\Lambda \to n\pi^0$.

Each step in Figures 15 and 16 involves certain operations. In Figure 15, I first perform a quark-antiquark production on a loop and next perform a charge switch on adjacent vertices. Then I move one end of an edge to

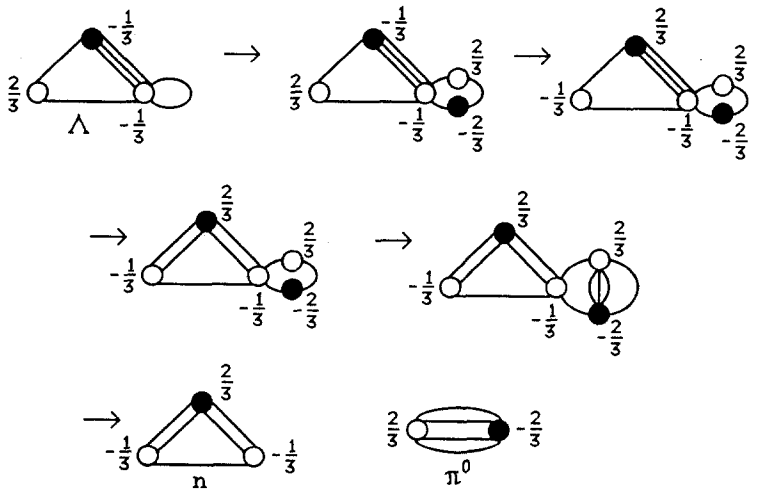

Fig. 16. $\Lambda \to n\pi^0$.

an adjacent vertex and perform this operation twice. Finally, I make two cuts. I do not consider the arcs between the lower right-hand vertex of the triangle and the vertices on the loop to be complete edges. Hence, after the cuts, the dangling ends disappear and do not need to be destroyed. These same operations are performed in Figure 16 together with an additional operation. In the next to last step, I create an edge on a loop and perform this operation three times. For more complicated decay processes, additional operations can occur. The admissible operations for weak baryon decay are the following.

1. Quark–antiquark production on a loop.
2. Edge cut.
3. Edge move to an adjacent vertex.
4. Edge creation on a loop.
5. Destroy edge after cut.
6. Charge switch on adjacent vertices.
7. Spin flip on a vertex.
8. Move loop to adjacent vertex.
9. Move loop to nonadjacent vertex.

The operations 7–9 can be performed at most once, while the other operations can be performed any number of times.

I now use the operations to compute branching ratios and decay probabilities. To do this one needs a quantitative measure of a particle's resistance toward decay along a specified channel. Roughly speaking, the greater the number of operations and the redundancy of operations, the more unlikely will be a decay along that channel. I postulate that each operation has a certain cost. Moreover, decay processes dislike redundancy, so repeated operations require additional costs. For a decay process $A \to BC$, the weak graph A transforms into the component weak graphs of B and C via admissible operations that minimize the total cost. The total cost, which is defined as the sum of the costs of the operations, is denoted $c(A \to BC)$.

The cost for one operation of type 9 is three units and the cost for one operation of any other type is one unit. For repeated operations of types 1–5 the cost sequence is $1, 3, 5, 7, \ldots$, while for repeated operations of type 6 the cost sequence is $1, 5, 9, 13, \ldots$. For example, if a type 4 operation is performed three times, then the cost for the first time is one unit, the second time is three units, and the third time is five units.

Denoting the mass of a particle X by m_x, I define the *mass difference* of the process $A \to BC$ by

$$\Delta m(A \to BC) = m_A - m_B - m_C$$

Suppose a particle A can decay along various channels $A \to B_i C_i$, $i = 1, \ldots, n$.

Denote the mass difference and cost of the ith channel by Δm_i, and c_i, respectively, $i = 1, \ldots, n$. I postulate that the *branching ratio* of the jth channel to the kth channel for a weak baryon decay is

$$r_{jk} = \frac{c_k \Delta m_k}{c_j \Delta m_j}$$

Moreover, the *decay probabilities*

$$P_i = P(A \to B_i C_i), \qquad i = 1, \ldots, n$$

satisfy $r_{jk} = P_j / P_k$. If it is known that $\sum_{i=1}^{n} P_i = 1$, then it easily follows that

$$P_j = \left[1 + \sum_{k=1}^{n} (r_{jk})^{-1} \right]^{-1}, \qquad j = 1, \ldots, n$$

Following tradition, I shall multiply decay probabilities by 100, so strictly speaking I am really referring to decay percentages.

Let us apply these ideas to the decay processes in Figures 15 and 16, which I designate as channels 1 and 2, respectively. Adding costs in the order of the steps of Figures 15 and 16, we have

$$c_1 = 1+1+1+3+1+3 = 10$$

$$c_2 = 1+1+1+1+3+5+1+3 = 16$$

Since

$$\Delta m_1 = m_\Lambda - m_p - m_{\pi^-} = 1115.6 - 938.3 - 139.6 = 37.3$$

$$\Delta m_2 = m_\Lambda - m_n - m_{\pi^0} = 1115.6 - 939.6 - 135 = 41$$

we have

$$r_{12} = \frac{c_2 \Delta m_2}{c_1 \Delta m_1} = \frac{16(41)}{10(37.3)} = 1.74 \; (1.79 \pm 0.04)$$

and

$$P_1 = \frac{1}{1 + (r_{12})^{-1}} = \frac{1.74}{2.74} = 63.5 \; (64.2 \pm 0.5)$$

$$P_2 = 36.5 \; (35.8 \pm 0.5)$$

where the numbers in parentheses are experimental values (Aguilar-Benitez *et al.*, 1986).

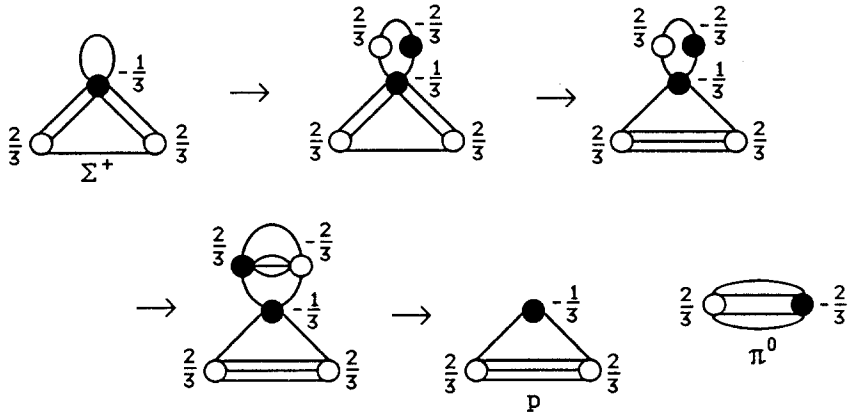

Fig. 17. $\Sigma^+ \to p\pi^0$.

Let us now consider other examples of weak baryon decay processes. The decay processes $\Sigma^+ \to p\pi^0$ and $\Sigma^+ \to n\pi^+$ are illustrated in Figures 17 and 18, respectively. The total costs become

$$c_1 = 1+1+3+1+3+5+1+3 = 18$$

$$c_2 = 1+1+5+9+1+3 = 20$$

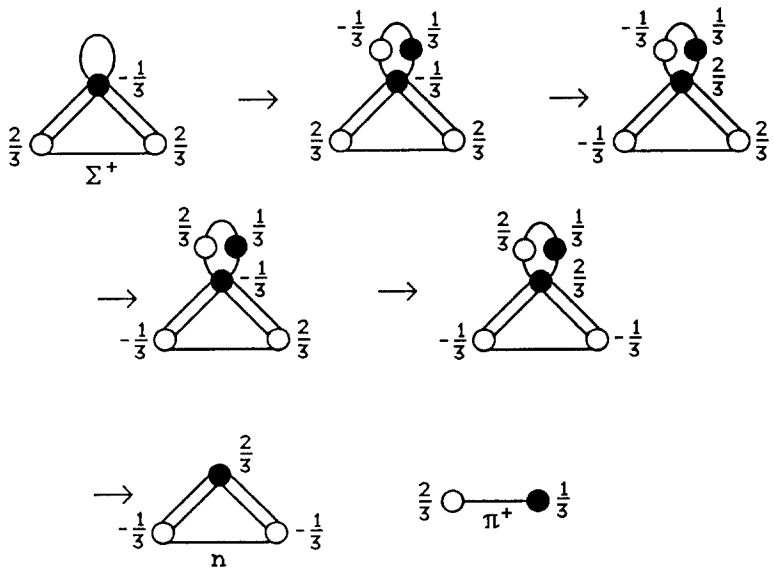

Fig. 18. $\Sigma^+ \to n\pi^+$.

We then have

$$r_{12}=\frac{c_2\Delta m_2}{c_1\Delta m_1}=\frac{20(110.2)}{18(116.1)}=1.055\ (1.068\pm 0.013)$$
$$P_1=51.34\ (51.64\pm 0.30)$$
$$P_2=48.66\ (48.36\pm 0.30).$$

The decay processes $\Omega\to K^-\Lambda$, $\Omega\to\Xi^0\pi^-$, and $\Omega\to\Xi^-\pi^0$ are illustrated in Figures 19–21, respectively. The total costs become

$$c_1=1+1+1+1+3+1+3+5+7+1=24$$
$$c_2=1+1+1+1+3+5+7+1=20$$
$$c_3=1+1+1+3+1+3+5+1+3+5+7+9+11+1+3=55$$

We then have

$$r_{12}=\frac{c_2\Delta m_2}{c_1\Delta m_1}=\frac{20(217.9)}{24(63.2)}=2.87\ (2.87\pm 0.05)$$
$$r_{13}=\frac{c_3\Delta m_3}{c_1\Delta m_1}=\frac{55(216.2)}{24(63.2)}=7.84\ (7.88\pm 0.42)$$
$$P_1=67.8\ (67.8\pm 0.7)$$
$$P_2=\frac{P_1}{r_{12}}=23.6\ (23.6\pm 0.7)$$
$$P_3=\frac{P_1}{r_{13}}=8.65\ (8.6\pm 0.4)$$

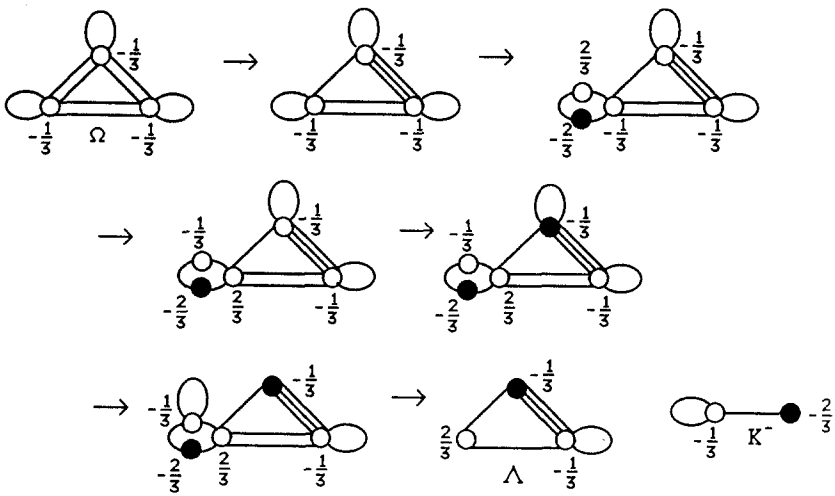

Fig. 19. $\Omega\to\Lambda K^-$.

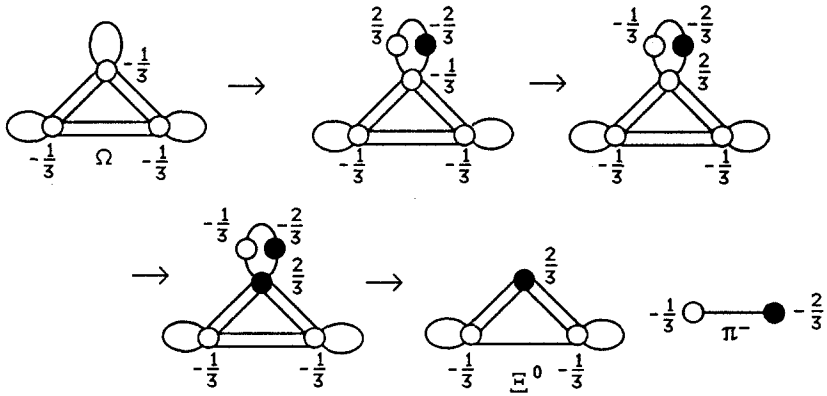

Fig. 20. $\Omega \to \Xi^0 \pi^-$.

5. WEAK MESON DECAY

If a node of a graph has charge 1/3 or −2/3, I call it an *antivertex* and if the node has charge −1/3 or 2/3, I call it a *vertex* as before. Of course, a baryon graph has three vertices or three antivertices, while a meson graph has a vertex and an antivertex. A loop on a vertex is again called a *loop*, while a loop on an antivertex will be called an *antiloop*. For a weak meson decay I postulate that vertices must remain vertices and antivertices

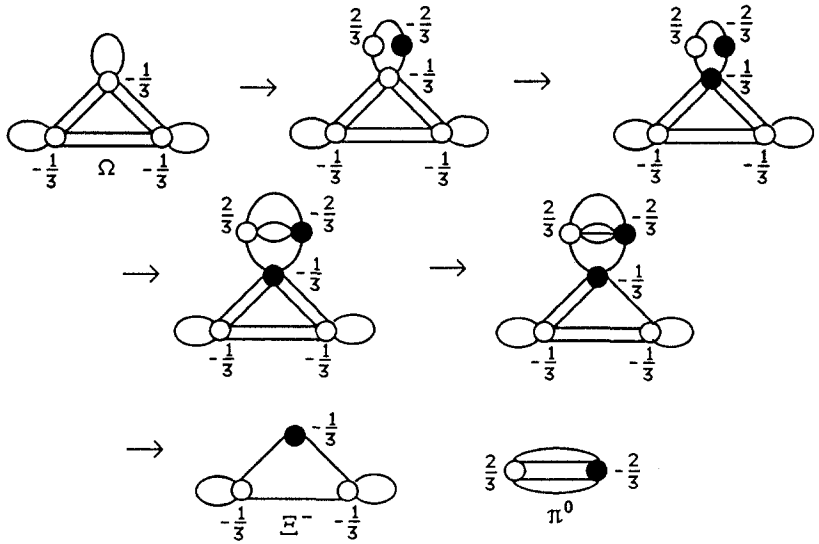

Fig. 21. $\Omega \to \Xi^- \pi^0$.

must remain antivertices. Thus, a charge switch cannot be applied if it changes a vertex to an antivertex or vice versa.

The operations for a weak meson decay are the same as for a weak baryon decay, except that we have two additional operations.

10. Loop or antiloop creation.
11. Move a charge of $\pm 2/3$ along an edge.

Operation 11 can be applied at most once. For weak meson decay, the costs of operations 1-9 are the same as for weak baryon decay except that a multiple edge can be destroyed at 0 cost (and repeated at 0 cost), it can be moved to an adjacent vertex to form a loop at 0 cost (and repeated at 0 cost) and it can be moved anywhere at a cost of one unit (and repeated at a cost of one unit). The cost of operation 11 is 1/3. For operation 10, suppose m loops and n antiloops are created. Then the total cost of these $m+n$ operations is

$$|1+2+\cdots+m-1-2-\cdots-n| = \tfrac{1}{2}|m(m+1)-n(n+1)|$$

In Section 4 we only considered weak baryon decays for which there were two decay products, since many of the important decay processes had this property. However, there are important weak meson decays with three decay products. The situation then becomes more complicated. Let $A \to BCD\ldots$ be a weak decay process. Assuming that neutrinos have zero mass, let n be the number of massive charged decay products, q the number of massive chargeless decay products, m the number of massless decay products, and $p = n+m+q$ the total number of decay products. We define the *mass factor* by

$$f(A \to BCD\ldots) = |1+(p-2)|\left[\frac{3n-5}{12} - \frac{9m}{16} + 6\binom{q}{3}\right]$$

where $\binom{q}{3} = q(q-1)(q-2)/6$. Of course, if there are two decay products, $f(A \to BC) = 1$ and we have the situation in Section 4.

I postulate that the *branching ratio* of the jth channel to the kth channel for a weak meson decay process is

$$r_{jk} = \frac{c_k f_j \Delta m_j}{c_j f_k \Delta m_k}$$

as before, the decay probabilities satisfy $r_{jk} = P_j / P_k$.

The decay processes $K^+ \to \mu\nu_\mu$, $K^+ \to \pi^0\pi^+$, $K^+ \to \pi^+\pi^+\pi^-$, $K^+ \to \pi^0\pi^0\pi^+$, $K^+ \to \pi^0 e\nu_e$, and $K^+ \to \pi^0\mu\nu_\mu$ are illustrated in Figures 22-27, respectively.

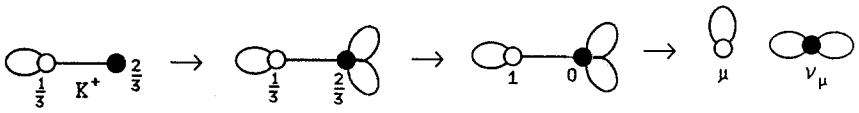

Fig. 22. $K^+ \to \mu \nu_\mu$.

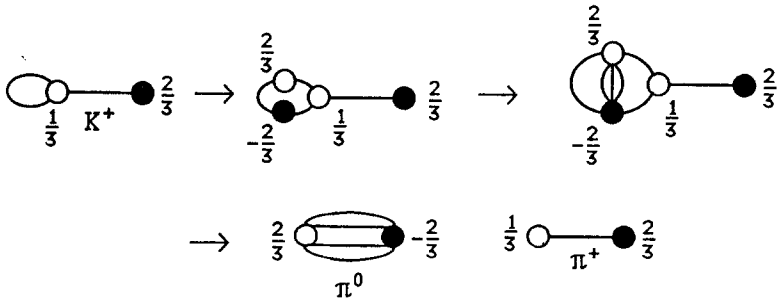

Fig. 23. $K^+ \to \pi^0 \pi^+$.

In Figures 24 and 25, a 2/3, −2/3 production is considered to be a different operation than a 1/3, −1/3 production. In the order given above, the total costs become

$$c_1 = 1+2+\tfrac{1}{3}+1+3+1 = 8\tfrac{1}{3}$$

$$c_2 = 1+1+3+5+1+3 = 14$$

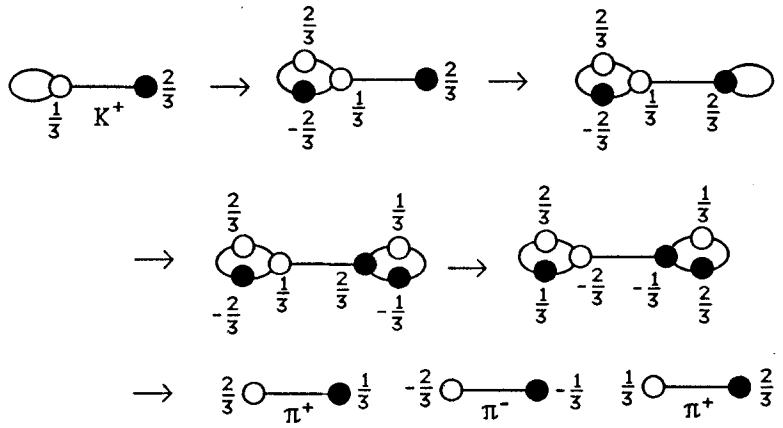

Fig. 24. $K^+ \to \pi^+ \pi^+ \pi^-$.

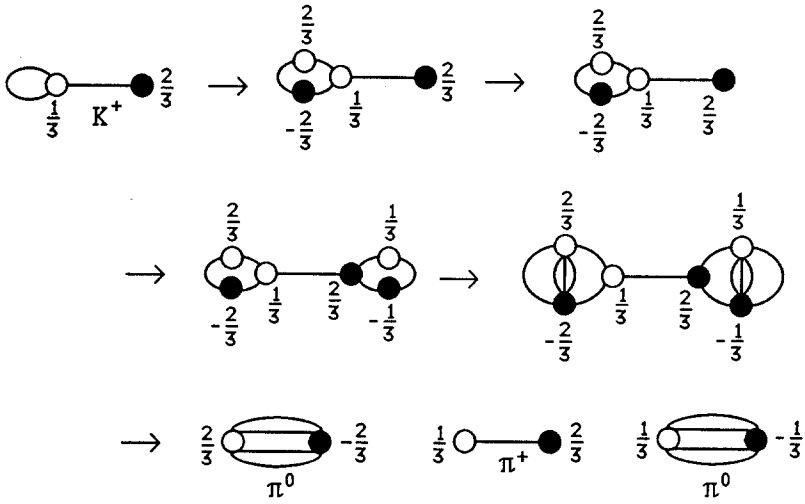

Fig. 25. $K^+ \to \pi^0\pi^0\pi^+$.

$$c_3 = 1+1+1+1+5+1+3+5+7 = 25$$
$$c_4 = 1+1+1+1+3+5+7+9+11+1+3+5+7 = 55$$
$$c_5 = 1+1+3+5+\tfrac{1}{3}+1+3+5+7+1 = 27\tfrac{1}{3}$$
$$c_6 = 1+1+2-1+\tfrac{1}{3}+1+3+5+1+3+5+7+1 = 29\tfrac{1}{3}.$$

The mass factors become

$$f_1 = f_2 = 1, \qquad f_3 = |1+\tfrac{1}{3}| = \tfrac{4}{3}, \qquad f_4 = |1-\tfrac{1}{6}| = \tfrac{5}{6}$$
$$f_5 = f_6 = |1-\tfrac{1}{6}-\tfrac{9}{16}| = \tfrac{13}{48}$$

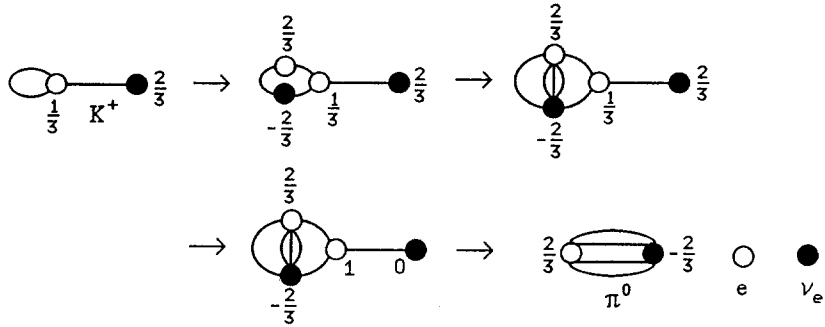

Fig. 26. $K^+ \to \pi^0 e \nu_e$.

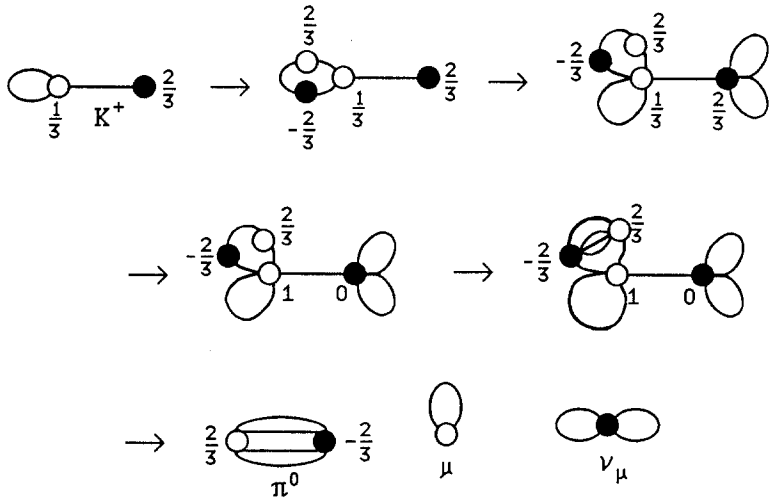

Fig. 27. $K^+ \to \pi^0 \mu \nu_\mu$.

We then have

$$r_{12} = \frac{c_2 f_1 \Delta m_1}{c_1 f_2 \Delta m_2} = \frac{14(388)}{8\frac{1}{3}(219.1)} = 2.98\ (3.00 \pm 0.03)$$

$$r_{13} = \frac{c_3 f_1 \Delta m_1}{c_1 f_3 \Delta m_3} = \frac{25(388)}{8\frac{1}{3}(\frac{4}{3})(74.9)} = 11.66\ (11.36 \pm 0.09)$$

$$r_{14} = \frac{c_4 f_1 \Delta m_1}{c_1 f_4 \Delta m_4} = \frac{55(388)}{8\frac{1}{3}(\frac{5}{6})(84.1)} = 36.5\ (36.7 \pm 0.2)$$

$$r_{15} = \frac{c_5 f_1 \Delta m_1}{c_1 f_5 \Delta m_5} = \frac{27\frac{1}{3}(388)}{8\frac{1}{3}(\frac{13}{48})(358.2)} = 13.12\ (13.18 \pm 0.17)$$

$$r_{16} = \frac{c_6 f_1 \Delta m_1}{c_1 f_6 \Delta m_6} = \frac{29\frac{1}{3}(388)}{8\frac{1}{3}(\frac{13}{48})(253)} = 19.9\ (20.0 \pm 0.7)$$

$$P_1 = \left[1 + \sum_{k=1}^{6} (r_{1k})^{-1}\right]^{-1} = 63.49\ (63.51 \pm 0.16)$$

$$P_2 = \frac{P_1}{r_{12}} = 21.30\ (21.17 \pm 0.15)$$

$$P_3 = \frac{P_1}{r_{13}} = 5.45\ (5.59 \pm 0.03)$$

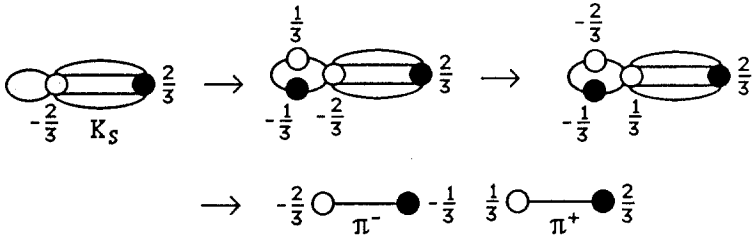

Fig. 28. $K_s \to \pi^-\pi^+$.

$$P_4 = \frac{P_1}{r_{14}} = 1.74\ (1.73 \pm 0.05)$$

$$P_5 = \frac{P_1}{r_{15}} = 4.84\ (4.82 \pm 0.05)$$

$$P_6 = \frac{P_1}{r_{16}} = 3.19\ (3.18 \pm 0.10).$$

The decay processes $K_S \to \pi^-\pi^+$ and $K_S \to \pi^0\pi^0$ are illustrated in Figures 28 and 29, respectively. The total costs become

$$c_1 = 1+1+0+0+0+1+3 = 6$$

$$c_2 = 1+1+3+5+1+3 = 14$$

Since $f_1 = f_2 = 1$, we have

$$r_{12} = \frac{c_2 f_1 \Delta m_1}{c_1 f_2 \Delta m_1} = \frac{14(218.5)}{6(227.7)} = 2.24\ (2.19 \pm 0.02)$$

$$P_1 = \frac{r_{12}}{1 + r_{12}} = 69.14\ (68.61 \pm 0.24)$$

$$P_2 = 30.86\ (31.39 \pm 0.24)$$

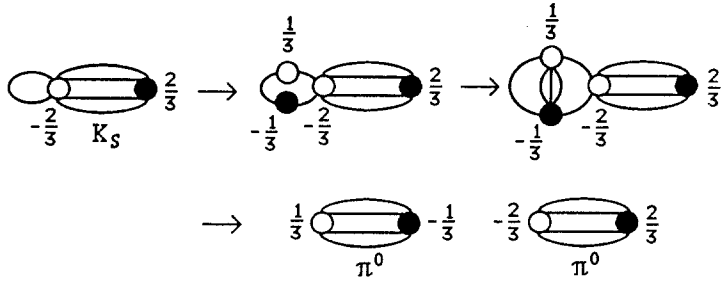

Fig. 29. $K_s \to \pi^0\pi^0$.

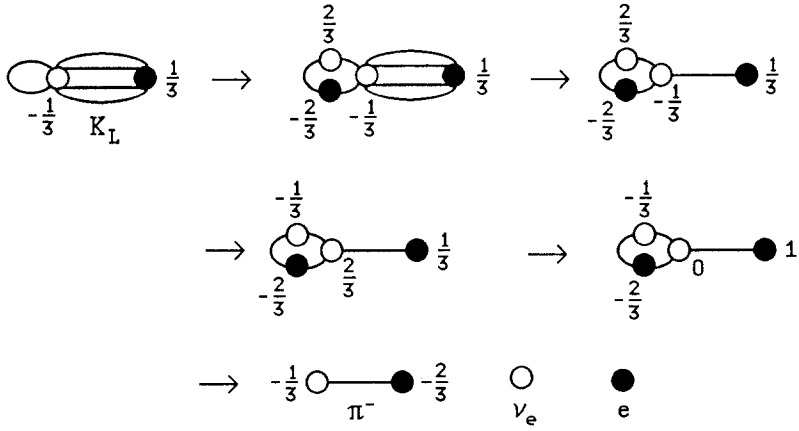

Fig. 30. $K_L \to \pi^- e \nu_e$.

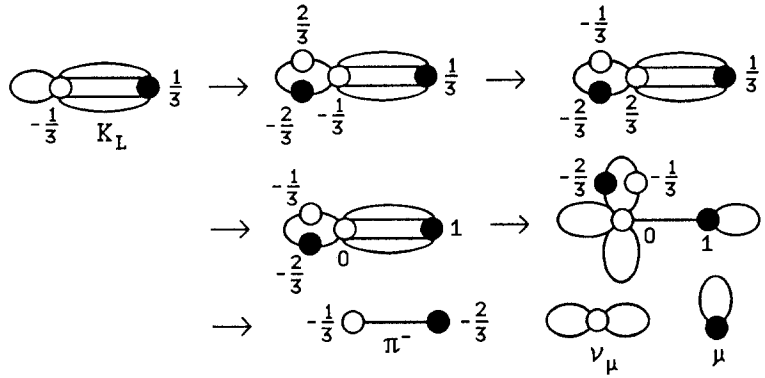

Fig. 31. $K_L \to \pi^- \mu \nu_\mu$.

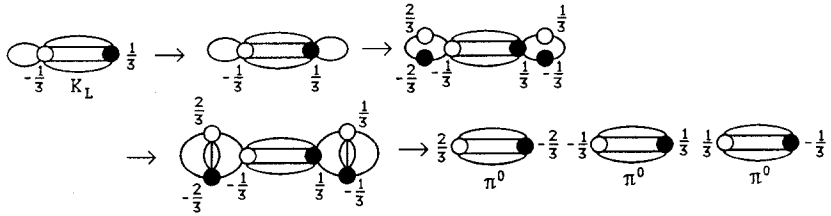

Fig. 32. $K_L \to 3\pi^0$.

The decay processes $K_L \to \pi^- e \nu_e$, $K_L \to \pi^- \mu \nu_\mu$, $K_L \to 3\pi^0$, $K_L \to \pi^+ \pi^+ \pi^0$ are illustrated in Figures 30–33, respectively. In Figure 33, the cuts on the four-edge pair $1/3$, $-1/3$ is considered to be different than the cuts on the one-edge pair $-1/3$, $2/3$. The total costs become

$$c_1 = 1+0+0+0+1+\tfrac{1}{3}+1+3+5+7+1 = 19\tfrac{1}{3}$$

$$c_2 = 1+1+\tfrac{1}{3}+0+0+0+1+3+5+7+1 = 19\tfrac{1}{3}$$

$$c_3 = 1+1+1+1+3+5+7+9+11+1+3+5+7 = 55$$

$$c_4 = 1+1+1+1+1+1+1+1+3+1+3 = 15.$$

The mass factors become

$$f_1 = f_2 = |1+\tfrac{1}{12}-\tfrac{9}{16}| = \tfrac{25}{48}$$

$$f_3 = |1-\tfrac{5}{12}+6| = 6\tfrac{7}{12}$$

$$f_4 = |1+\tfrac{1}{12}| = 1\tfrac{1}{12}$$

We then have

$$r_{12} = \frac{c_2 f_1 \Delta m_1}{c_1 f_2 \Delta m_2} = \frac{\Delta m_1}{\Delta m_2} = \frac{357.6}{251.9} = 1.42\ (1.43 \pm 0.09)$$

$$r_{13} = \frac{c_3 f_1 \Delta m_1}{c_1 f_3 \Delta m_3} = \frac{55(\frac{25}{48})(357.6)}{19\frac{1}{3}(6\frac{7}{12})(92.7)} = 0.868\ (0.900 \pm 0.076)$$

$$r_{14} = \frac{c_4 f_1 \Delta m_1}{c_1 f_4 \Delta m_4} = \frac{15(\frac{25}{48})(357.6)}{19\frac{1}{3}(1\frac{1}{12})(83.5)} = 1.60\ (1.56 \pm 0.08)$$

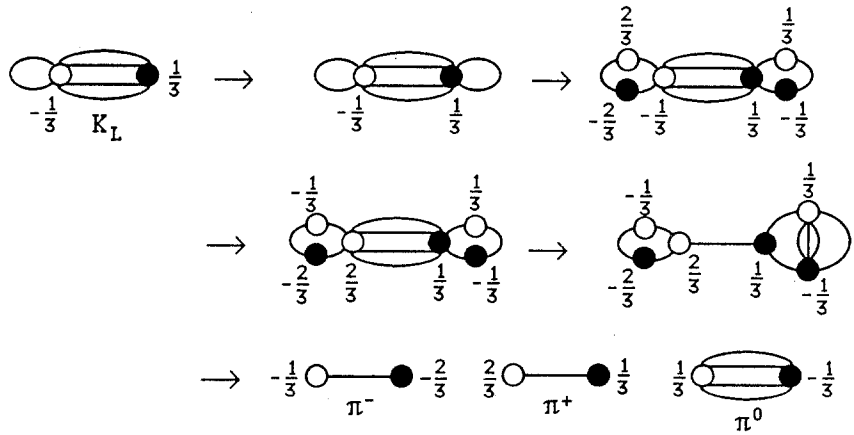

Fig. 33. $K_L \to \pi^+ \pi^0$.

We also have the processes $K_L \to \pi^+ e\nu_e$, and $K_L \to \pi^+ \mu\nu_\mu$, which have the same branching ratios and decay probabilities as $K_L \to \pi^- e\nu_e$ and $K_L \to \pi^- \mu\nu_\mu$, respectively. If we call these processes 5 and 6, respectively, we have

$$P_1 = P_5 = \left[1 + \sum_{k=1}^{6} (r_{1k})^{-1}\right]^{-1} = 19.3\ (19.4 \pm 0.6)$$

$$P_2 = P_6 = \frac{P_1}{r_{12}} = 13.6\ (13.6 \pm 0.4)$$

$$P_3 = \frac{P_1}{r_{13}} = 22.2\ (21.5 \pm 1.0)$$

$$P_4 = \frac{P_1}{r_{14}} = 12.1\ (12.4 \pm 0.2).$$

6. STRONG BARYON DECAY

The admissible operations for strong baryon decay processes are the following.

1. Quark-antiquark production on pairs of excitation vertices.
2. Quark-antiquark production on adjacent edges.
3. Edge cut.
4. Edge move to adjacent vertex.
5. Destroy edge after cut.
6. Spin flip on a vertex.
7. Reattach cut edge.
8. Destroy excitation vertex.

The cost sequence for edge cuts is $1, 2, 3, \ldots$. There is no additional cost for repeated operations of any other type. The cost for an operation of type 1 is 1 unit and for types 5 and 6 the cost is zero. For type 2 operations, if the edges have not been moved, the cost is 1 unit; otherwise, if the moved edge is a basic edge, then the cost is 4 units and if the moved edge is an excitation edge, then the cost is 16 units. For type 4 operations, if the edge move forms a double edge, the cost is 4 units and otherwise it is 1 unit. The cost for operations of types 7 and 8 is 8 units.

The mass factor is

$$f(A \to BC\ldots) = 1 + \binom{p}{3} + 3l$$

where p is the number of decay products and l is the total number of loops in the decay products. The channel ratio is defined to be $r_{12} = c_2 f_2 / c_1 f_1$ if the underlying basic baryon has spin 1/2 and $r_{12} = c_2 f_1 / c_1 f_2$ if the underlying basic baryon has spin 3/2. Figures 34 and 35 illustrate the strong processes

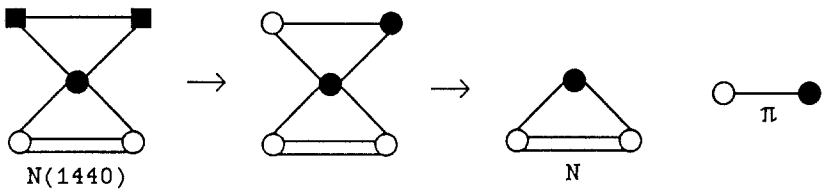

Fig. 34. $N(1440) \to N\pi$.

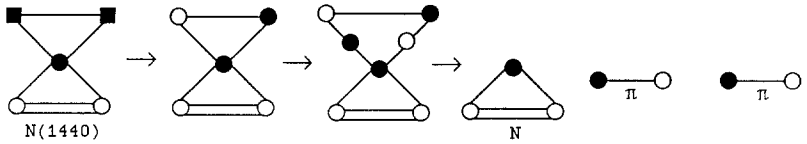

Fig. 35. $N(1440) \to N\pi\pi$.

$N(1440) \to N\pi$ and $N(1440) \to N\pi\pi$, respectively. As in some of the weak decay processes, there are two different kinds of edge cuts in Figure 35. We then have

$$c_1 = 1+1+2+3+4 = 11$$
$$c_2 = 1+1+1+2+1+2 = 8$$
$$f_1 = 1, \qquad f_2 = 2$$

Hence,

$$r_{12} = 16/11 = 1.45$$
$$P_1 = 1.45/2.45 = 59\ (50\text{-}70)$$
$$P_2 = 41\ (30\text{-}50)$$

Figures 36 and 37 illustrate the strong processes $N(1520) \to N\pi$ and $N(1520) \to N\pi\pi$, respectively. The total costs and mass factors become

$$c_1 = 1+1+1+2+3+4+5+6 = 23$$
$$c_2 = 1+1+1+2+3+4+1+2 = 15$$
$$f_1 = 1, \qquad f_2 = 2.$$

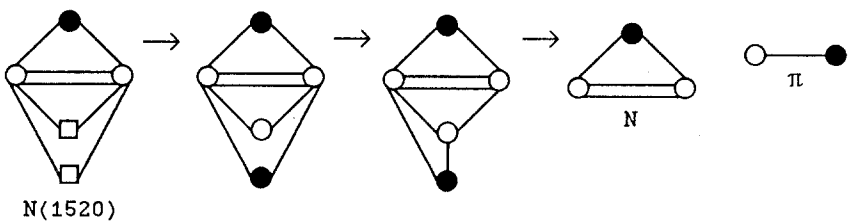

Fig. 36. $N(1520) \to N\pi$.

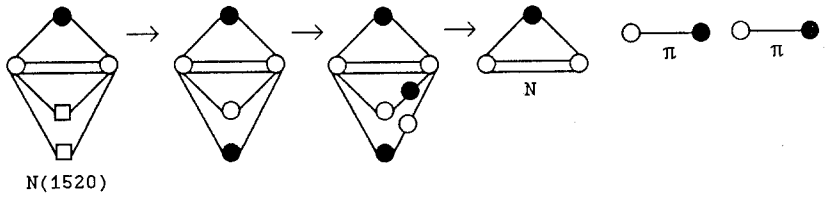

Fig. 37. $N(1520) \to N\pi\pi$.

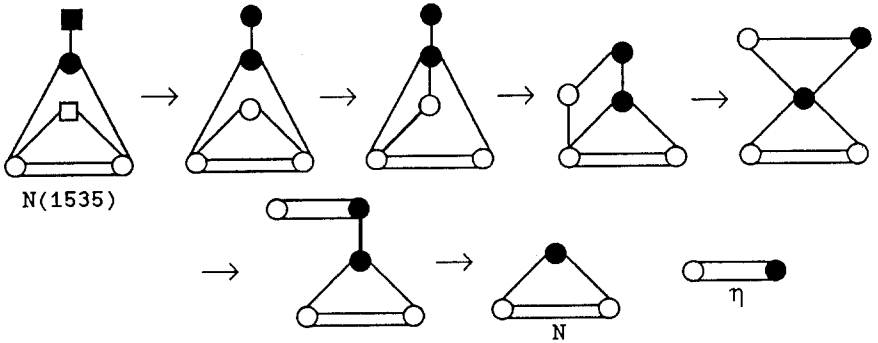

Fig. 38. $N(1535) \to N\eta$.

Hence,

$$r_{12} = 30/23 = 1.30$$

$$P_1 = 1.30/2.30 = 57\ (50\text{-}60)$$

$$P_2 = 43\ (40\text{-}50).$$

Figures 38-40 illustrate the strong processes $N(1535) \to N\eta$, $N(1535) \to N\pi$, $N(1535) \to N\pi\pi$, respectively. In Figures 39 and 40, the first four steps

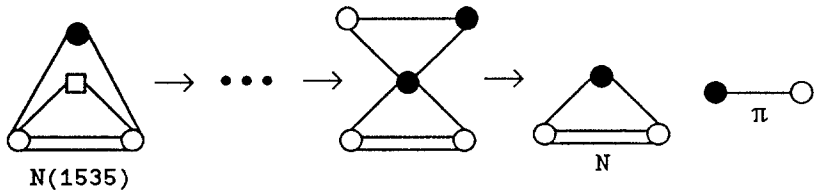

Fig. 39. $N(1535) \to N\pi$.

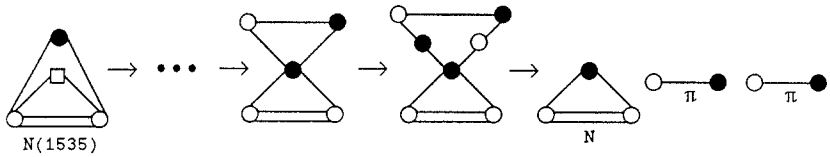

Fig. 40. $N(1535) \to N\pi\pi$.

are the same as in Figure 38. The total costs and mass factors become

$$c_1 = 1+1+1+1+4+1+2 = 11$$
$$c_2 = 1+1+1+1+1+2+3+4 = 14$$
$$c_3 = 1+1+1+1+16+1+2+1+2 = 26$$
$$f_1 = f_2 = 1, \qquad f_3 = 2$$

Hence,

$$r_{12} = \tfrac{14}{11} = 1.27$$
$$r_{13} = \tfrac{52}{11} = 4.73$$
$$P_1 = [1+(r_{12})^{-1}+(r_{13})^{-1}]^{-1} = 50\ (45\text{-}55)$$
$$P_2 = \frac{P_1}{r_{12}} = 39\ (35\text{-}50)$$
$$P_3 = \frac{P_1}{r_{13}} = 11\ (\sim 10)$$

Figures 41-43 illustrate the strong processes $N(1650) \to N\pi$, $N(1650) \to N\pi\pi$, $N(1650) \to \Lambda K$. The total costs and mass factors become

$$c_1 = 1+1+1+2+3+4+5+6+8+8+1+2+3+4+5+6 = 60$$
$$c_2 = 1+1+1+1+2+3+4+5+6+7+8+9+10 = 58$$
$$c_3 = 1+1+1+2+3+4+5+6+8+8+8+1+2+3+4 = 65$$
$$f_1 = 1, \qquad f_2 = 2, \qquad f_3 = 7.$$

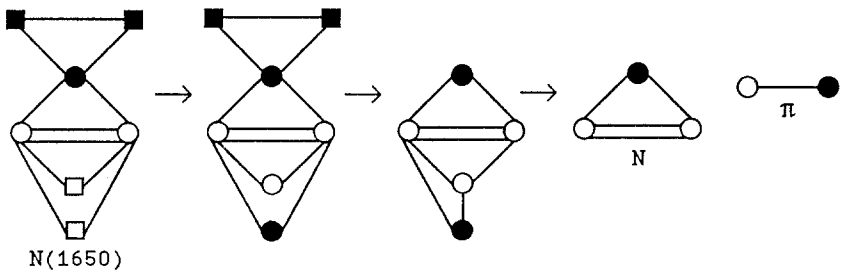

Fig. 41. $N(1650) \to N\pi$.

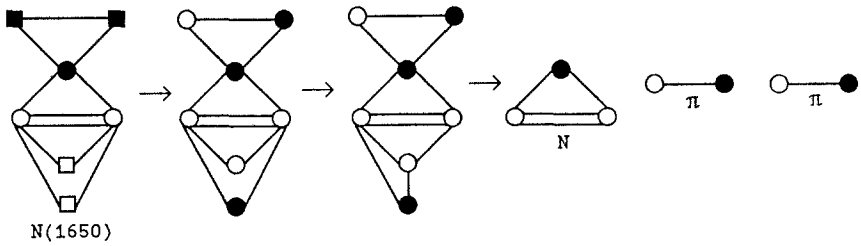

Fig. 42. $N(1650) \to N\pi\pi$.

Hence,

$$r_{12} = \frac{2(58)}{60} = 1.93$$

$$r_{13} = \frac{7(65)}{60} = 7.58$$

$$P_1 = [1 + (r_{12})^{-1} + (r_{13})^{-1}]^{-1} = 61 \text{ (55-65)}$$

$$P_2 = \frac{P_1}{r_{12}} = 31 \text{ (20-35)}$$

$$P_3 = \frac{P_1}{r_{13}} = 8(\sim 8)$$

Figures 44 and 45 illustrate the strong processes $\Delta(1620) \to N\pi\pi$ and $\Delta(1620) \to N\pi$. The total costs and mass factors become

$$c_1 = 1+1+4+1+2+3+4+1+2 = 19$$

$$c_2 = 1+1+1+1+2+3+4+5+6 = 24$$

$$f_1 = 1, \qquad f_2 = 2$$

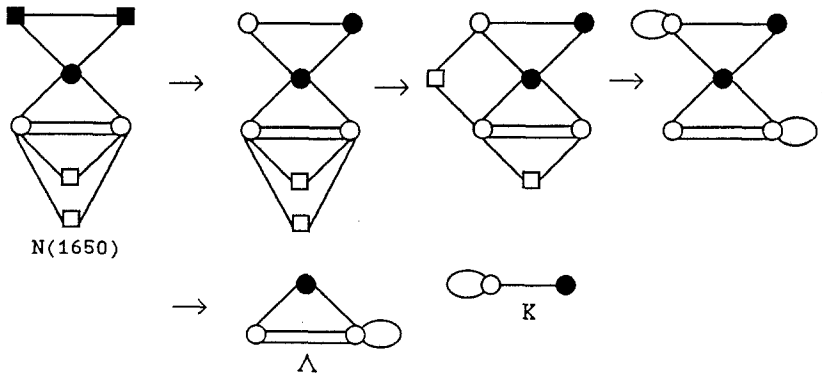

Fig. 43. $N(1650) \to \Lambda K$.

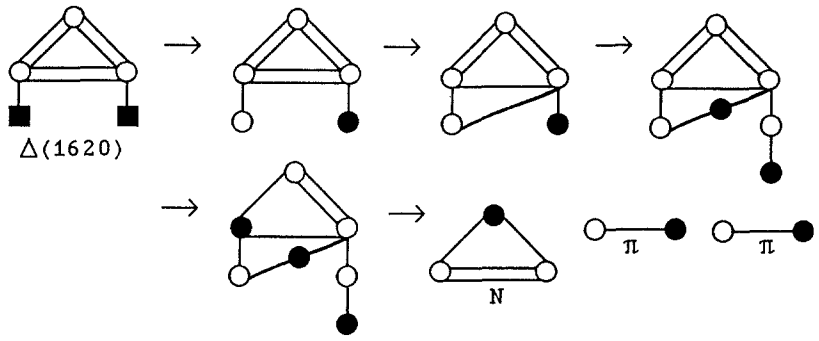

Fig. 44. $\Delta(1620) \to N\pi\pi$.

Hence,

$$r_{12} = 48/19 = 2.53$$

$$P_1 = 2.53/3.53 = 72\ (65\text{-}75)$$

$$P_2 = 28\ (25\text{-}35)$$

7. REMARKS

The particle decay model presented here not only gives quantitative predictions, it gives a qualitative way of "seeing" how a decay process takes place. Of course, I have only considered a few examples from among the vast number of possible decay processes. In particular, I have not considered decay processes for which there is essentially only one decay channel. An important example is the neutron β-decay exhibited in Figure 46.

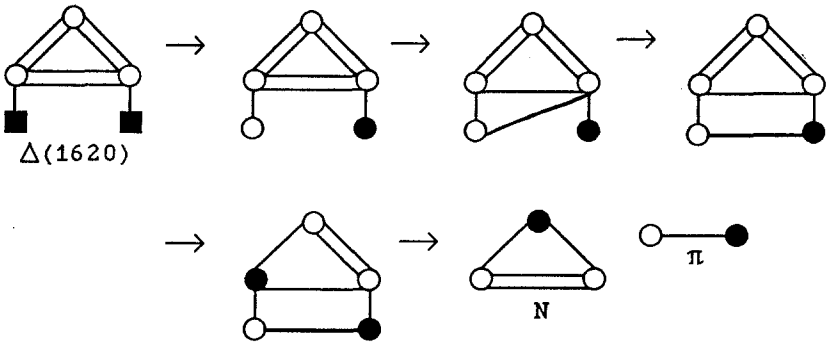

Fig. 45. $\Delta(1620) \to N\pi$.

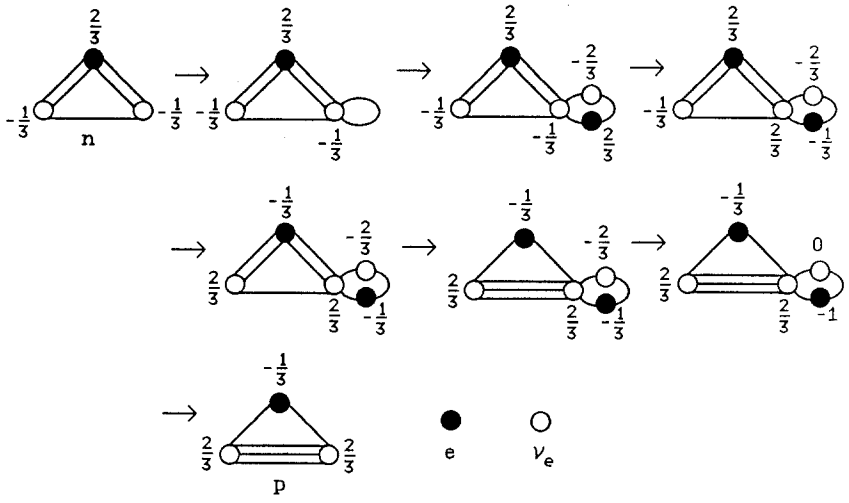

Fig. 46. $n \to pe\nu_e$.

Although the model presented here gives some predictions, it leaves many unanswered questions. For example, it does not address the question of why certain decay channels are suppressed. Moreover, it does not predict the very small branching ratios and decay probabilities for these suppressed channels. For instance, it does not answer why the processes $\Lambda \to pe\nu_e$, $\Lambda \to p\mu\nu_\mu$ and $\Lambda \to p\pi^-\delta$ are suppressed and why they have the incredibly small decay probabilities 8.35×10^{-4}, 1.57×10^{-4}, and $8.5 \times 10^{-4}(\%)$, respectively. As another example, I have neglected the process $N(1650) \to N\eta$ in Section 6. I do not know why this process is suppressed and only has probability 1.5%. Presumably, there are rules or conservation laws that inhibit these processes. Two other questions the model does not answer are the following. When have we found all the significant channels so that their probabilities sum to approximately 1? Why does K_s decay differently than K_L?

REFERENCES

Aguilar-Benitez, M., *et al.* (Particle Data Group) (1986). Review of particle properties, *Physics Letters B*, **170B**, 1-342.

Gudder, S. (1988). Finite model for particles, *Hadronic Journal*, **11**, 21-34.